Short Communication

Propellants, Explosives, Pyrotechnics

doi.org/10.1002/prep.202100239

Thermal Decomposition of Photocurable Energetic APNIMMO Polymer

Weitao Yang,*[a, b] Rui Hu,[b] Manman Li,[b] Minghui Xu,[b] Zhiwei Yang,[a] and Lingjie Meng[a]

Abstract: Photocurable energetic polymer contains energetic groups (explosophores) and provides fast curable property for 3D printed propellants. Acrylate-terminated poly-3-nitratomethyl-3-methyloxetane (APNIMMO) was prepared for the stereolithography (SLA) printing. This work outlines the thermal decomposition process of APNIMMO. The thermal behaviour and decomposition kinetics were investigated by means of the non-isothermal DSC (differential scanning calorimetry) techniques. The Arrhenius parameters were studied by different isoconversional Kissinger method. Additionally, simultaneous TG-DSC-FTIR-MS were employed to corroborate the thermal analysis results. The obtained results from the different techniques are presented and discussed.

Keywords: Energetic polymer · APNIMMO · Thermal behaviors · Decomposition kinetics

1 Introduction

In recent years, 3D extrusion printing [1,2], digital light processing (DLP) [3,4] and stereolithgraphy (SLA) [5,6] have been adpted to printing propellants or explosives. In 3D printing process, binders always play an important role to improve the mechanical properties and participates in redox reactions with other components [7]. In view of inherent disadvantages of inert binders (such as degraded thermodynamic energy and burning residue), there has been profound interest to develop energetic polymer as suitable candidate for binder applications.

Energetic polymers contain energetic groups (explosophores) such as the nitro-, nitrato-, azido-, etc. The use of these binders is aimed at developing high-energy, smokeless, explosion-proof and low vulnerability composite energetic systems [8,9]. A various of papers report on the synthesis procedures and properties of promising azido polymers such as GAP [10], PBAMO [11], and polymers with nitrate groups, namely, polyGLYN and NIMMO [12]. These energetic binders are cross-linked by chemical curing/cross-linking agents such as TDI or MDI for hours which are not suitable for 3D printing [13].

Researchers [14,15] dissolved nitrocellulose/nitroglycerine carpets in ethyl acetate or alcohol/ketone solvent for 3D extrusion printing. This method needed a long time to remove the solvent after printing. Fraunhofer ICT [16] investigated GAP-based EPTE as binder that can be processed according to the Fused Deposition Modeling (FDM) method without using solvent. TNO working on additive manufacturing from 2013 and developed photocurable energetic composites composed of inert acrylates, energetic solid filler, and energetic plasticizer for vat photopolymerization additive manufacturing [17–20]. All the trials verified the feasibility of using photocurable resins in 3D printing of the propellants. In order to improve the combustion performance of the photocurable composites, the acrylates containing explosophores are needed. Sagi Sevilia [21] prepared photocurable energetic mono- and bisvinylimidazolium perchlorate salts and demonstrated the printability of this material. In our previous study [22], we synthesized a novel halogen-free energetic photocurable oligomer (acrylate-terminated poly-3-nitratomethyl-3-methyloxetane, abbreviated as APNIMMO) which could be fast cured under UV (ultraviolet) light, including the synthesis, structure characterization and demonstration of the SLA 3D printing. The new binder presented excellent performance in promoting the energy content and burn rate of a propellant.

Based on the previous study, this paper will discuss the thermal behavior and decomposition kinetics of APNIMMO binder. Herein, APNIMMO were prepared and the thermal decomposition behavior, including the kinetic parameters were investigated. The results will help understand the thermal properties of the new developed binder, which could provide more information for 3D printed propellants or explosives.

[a] *W. Yang, Z. Yang, L. Meng*
School of Physics
Xi'an Jiaotong University
Xi'an, 710049, PR China
**e-mail: njyangweitao@163.com*
[b] *W. Yang, R. Hu, M. Li, M. Xu*
Xi'an Modern Chemistry Research Institute
Xi'an, 710065, PR China

2 Experiment Section

2.1 Materials and Manufacturing Process

The binder matrix was prepared by mixing poly-3-nitratomethyl-3-methyloxetane (APNIMMO) and trimethylolpropane trimethacrylate (TMPTA) in a mass ratio of 7:3. 2,4,6-trimethylbenzoyl diphenyl phosphine oxide (TPO) was used as photo initiator. Acrylate-terminated APNIMMO oligomer was inhouse production (shown in Figure 1) and the detailed synthesis process could be found in our previous published paper [22]. The polymer binder was cured under a 405 nm UV light for 10 s.

2.2 Differential Scanning Calorimetry (DSC)

The cured APNIMMO was tested by Mettler-Toledo HP DSC 827e. The temperature range of 50–300 °C and the heating rates were 5, 10, 15 and 20 °C min^{-1} in dynamic nitrogen atmosphere (ca. 50 mL min^{-1}).

The activation energy E_a was calculated by the Kissinger method (Eq.1) and modified Kissinger-Akahira-Sunose (KAS) method (Eq.2) which is described as below [23, 24].

$$\ln\left(\frac{\beta}{T_p^2}\right) = \ln\left(\frac{AR}{E_a}\right) - \frac{E_a}{R\,T_p} \quad (1)$$

Where β is the heating rate and T_p is the peak temperature of the exothermic peak at that rate; α is the extent of conversion. The activation energy is calculated from the slope of $\ln(\beta/T_p^2)$ against $1/T_p$ curves, and pre-exponential factor, A_k is obtained by the intercept.

$$\ln\left(\frac{\beta}{T_\alpha^{1.92}}\right) = const - 1.0008\frac{E_\alpha}{R\,T_\alpha} \quad (2)$$

Where α is the extent of conversion, the activation energy is calculated from the slope of $\ln\left(\frac{\beta}{T_\alpha^{1.92}}\right)$ against $(1/T_\alpha)$ line at different extent of conversions.

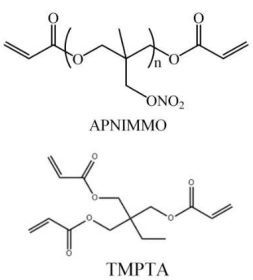

Figure 1. Structure of APNMMO oligomer and TMPTA.

2.3 TG-DSC–MS-FTIR Analysis

TG-DSC-FTIR analysis was performed on instruments STA8000-Spectrum 3-Clarus690 SQ8C, PerkinElmer. Approximately 2 mg of APNIMMO was heated from 50 °C to 400 °C at a heating rate of 5 °C min^{-1}. The volatile products from DSC/TG were analyzed on-line by MS and FTIR.

3 Results and Discussion

3.1 Thermal Analysis Study of APNIMMO Binder

Figure 2 presents the DSC curves obtained at heating rates of 5, 10, 15 and 20 °C min^{-1}. The enthalpies of decomposition of APNIMMO are determined by integrating the area under the exothermic peaks, assuming a linear baseline. It is clear that the onset temperature of all sample increased with increasing of the heating rate. The peak temperature of exothermic peaks is 213.7, 219.2, 226.5 and 229.6 °C at heating rate of 5, 10, 15 and 20 °C min^{-1}, respectively. The decomposition temperature range and exothermic peak are very similar to that of poly(3-nitratomethyl-3-methyloxetane) (PNIMMO) reported before ascribed to the thermal decomposition of $-ONO_2$ [25, 26].

The Arrhenius parameters for the thermal decomposition of APNIMMO calculated by Kissinger method are listed in Table 1. The calculated activation energy E_a was 159.8 kJ mol^{-1} and the ln of the pre-exponential factor ($\ln(A_k)$) was 45.4. The activation energy is also similar to PNIMMO.

3.2 Dependence of Kinetic Parameters on Extent of Conversion

The dependence of the conversion extent on the temperature (α-T) curves APNIMMO is shown in Figure 3. The de-

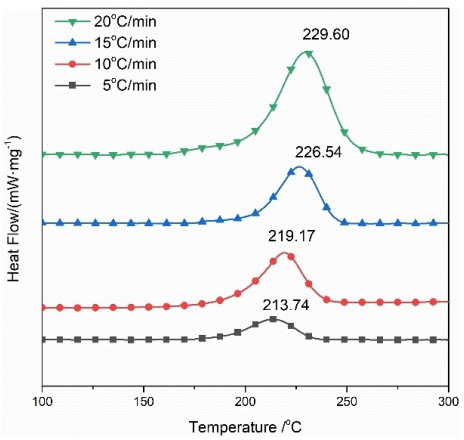

Figure 2. DSC curves of pure APINIMMO at defferent heating rates.

Table 1. Kinetic parameters of APNIMMO compared with PNIMMO polymer.

Polymer	Heating rate β [°C min^{-1}]	Exothermic Peaks				Arrhenius parameters	
		T_0 [°C]	T_p [°C]	T_c [°C]	ΔH [kJ/g]	E_a [kJ·mol^{-1}]	lnA_k
APNIMMO	5	169.7	213.7	242.9	1.16	159.8	45.4
	10	173.0	219.2	253.1	1.25		
	15	181.4	226.5	260.7	1.30		
	20	181.3	229.6	265.6	1.32		
PNIMMO [27]	2.5	–	199.8	–	–	168.1	36.84
	5	–	206.8	–	–		
	10	–	213.6	–	–		
	20	–	223.0	–	–		

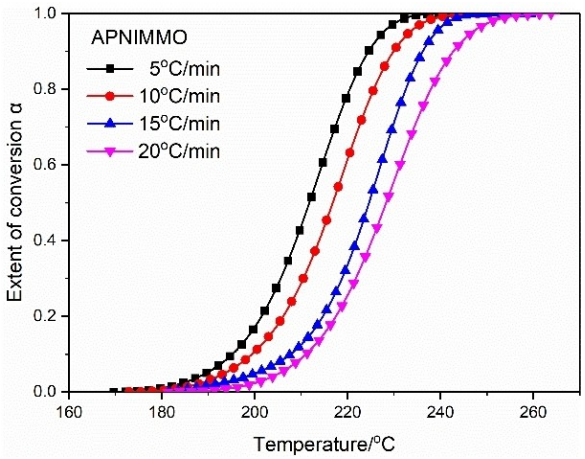

Figure 3. The α-T curves of APNIMMO at different heating rates.

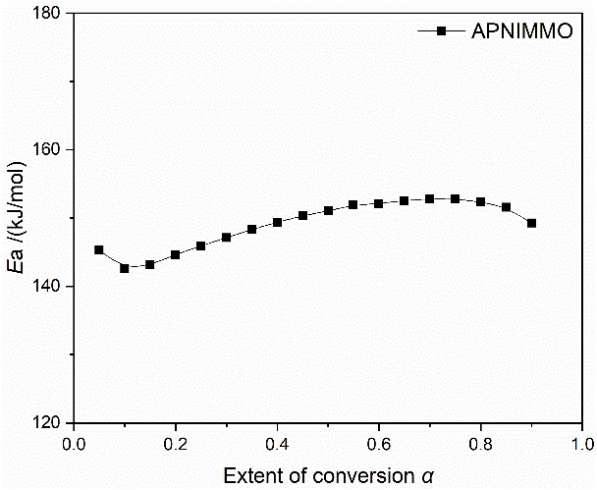

Figure 4. Dependence of activation energy on extent of conversion of APNIMMO by isoconversional modified KAS method.

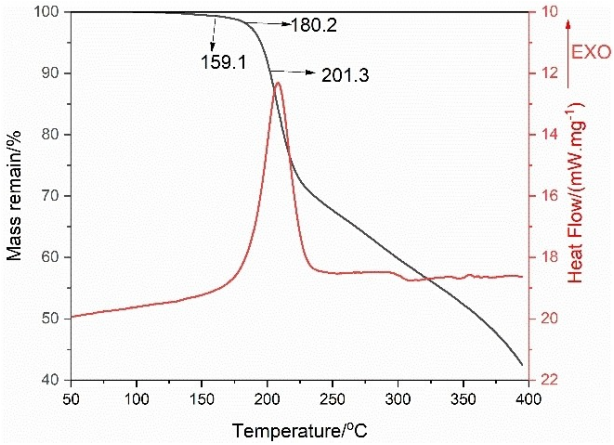

Figure 5. TG and DSC curves of APNIMMO at heating rate of 5 °C/min.

pendence of the activation energy on the extent of conversion calculated by KAS method is presented in Figure 4. The activation energy of 147.7 ± 5.1 kJ mol^{-1} was obtained ($0.5 < \alpha < 0.95$). The activation energies obtained from KAS method is slightly lower than and the investigation of activation energy using Kissinger method.

3.3 TG-DSC-FTIR Analysis

TG-DSC-FTIR analysis was performed to analyze the volatile gas released at the heating rate of 10 °C min^{-1} during decomposition. The DSC/TG curve is shown in Figure 5. The TG curve shows a two-step decomposition with a turning point of ~220 °C with a mass loss of 28 %. Meanwhile, the gas products were taken away from TG pans to FTIR and MS, and the oxidation effect of gas products with residues was weakened, resulting a mass loss without exothermic or endothermic peaks in DSC curves.

Figure 6 presents the FTIR spectral data, including absorbance, wavenumber, and time, of the volatile gas from the pyrolysis of APNIMMO. The major products of decomposition resulting from this isothermal study were identified by FTIR. The main absorption peaks of volatiles in the pyrolysis ranged from 159.1 °C to 201.3 °C. The absorbance peak of N_2O (2238 cm^{-1}) and CO (2176 cm^{-1}) generated at ~160 °C and disappeared at ~201 °C with a weight loss of 9.1 %. It reveals the initial decomposition of APNIMMO is the scission of O–NO_2 bond. But NO_2 (~1600 cm^{-1}) was not found in the FTIR spectrum. Unreacted TMPTA during 3D printing volatilized at ~1000 s (~83 °C), posing a disturb for judge the absorbance intensity change. Figure 7 presents subtracted FTIR spectrums of 180.2, 201.3 and 224.1 °C by 159.1 °C to compare the absorbance change of the generated products. N_2O, NO and CH_2O was generated at 180.1 °C, and these products disappeared at 201 °C.

Figure 8 presents the MS results and Table 2 lists the m/Z ratio with the corresponding temperatures, including de-

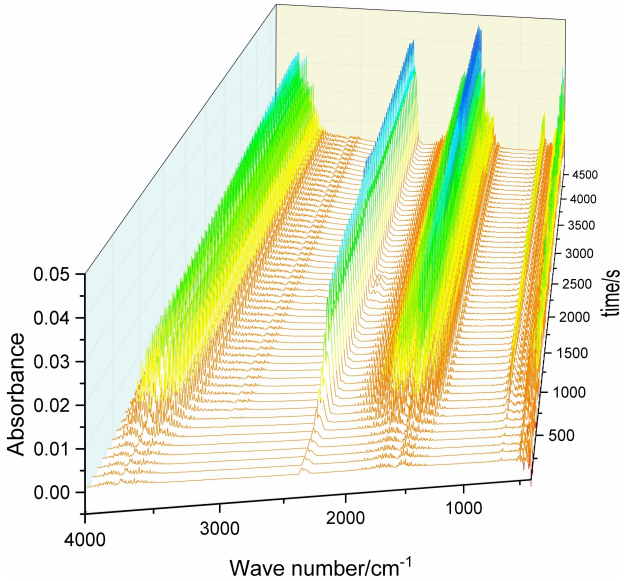

Figure 6. FTIR spectrum for gas products with time heated in helium at 5 °C min^{-1}.

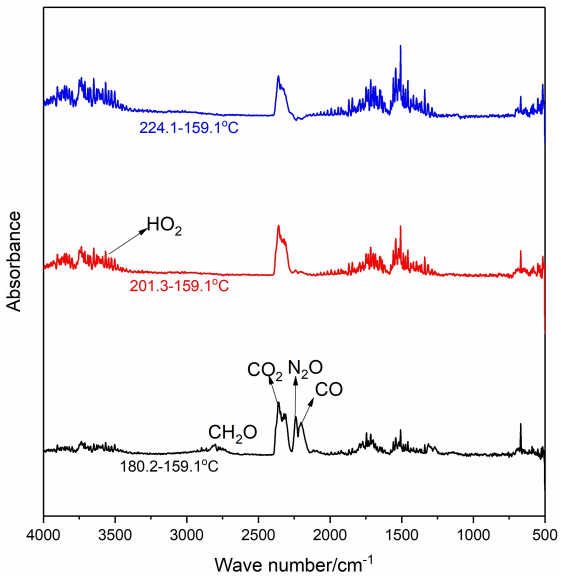

Figure 7. Subtracted FTIR spectrums of 180.2, 201.3 and 224.1 °C by 159.1 °C.

tected temperature range (T_0-T_e) and maximum intensity temperature (T_p). In the MS results shown in Figure 8, mass-to-charge ratio (m/Z) of 17 (NH_3), 18 (H_2O), 28 (CO), 30 (NO, CH_2O), 43 (HCNO) and 44 (N_2O, CO_2) were detected. NO, CH_2O was first found at ~128 °C, followed by HCNO, CO_2, N_2O, H_2O and CO.

The NO_2 is hard to detect in FTIR and MS tests resulting from the evolved NO_2 may decompose or combine with substaintial generated CH_2O from the side chain as shown in Scheme 1 [28]. Table 2 also reveals the generation of NO

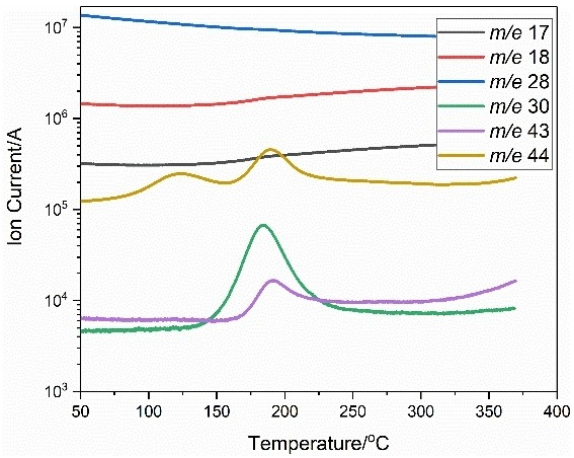

Figure 8. MS results for ~2 mg APNIMMO heated in helium at 5 °C min^{-1} to 350 °C.

Table 2. m/Z ratio and the corresponding temperatures.

m/Z	T_0~T_e [°C]	T_p [°C]	Possible assignment
17	165~232	188	NH_3
18	161~210	187	H_2O
28	171~226	188	CO
30	128~258	184	NO, CH_2O
43	148~253	191	HCNO
44	156~244	189	CO2, N_2O

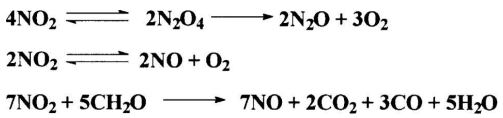

Scheme 1. Decomposition and reaction of nitro groups.

is 28 °C before N_2O generation, revealing the oxidation reaction of NO_2 with CH_2O. The FTIR spectrum and MS results are consistent with the mass loss rule of the TG/DSC curve. The weight loss and FTIR results for this study can to a certain extent verify this degradation before 201 °C (before the exothermic peak in DSC curve) involving the homolytic scission of the O–NO_2 bond resulting in the loss of nitro group and the subsequent loss of CH_2O from the polymer side chain. The generated gas products react with each other and the main final products are N_2O, CO_2, CO and H_2O.

4 Conclusions

The thermal decomposition of APNIMMO has a two-step decomposition process. Before 201.3 °C, the main degradation mainly contains the scission of the O–NO_2 bond resulting in the loss of nitro group and the subsequent loss of formaldehyde (CH_2O) from the polymer side chain. Pyrolysis

of the residues mainly generate CO_2, H_2O and hydrocarbons. The kinetic parameters are obtained by the Kissinger method and modified Kissinger-Akahira-Sunose (KAS) method. The activation energy is 159.8 kJ/mol^{-1}, which is very similar to that of polyNIMMO.

Data Availability Statement

Research data are not shared.

References

[1] M. S. McClain, I. E. Gunduz, S. F. Son, Additive manufacturing of ammonium perchlorate composite propellant with high solids loadings, *Proceedings of the Combustion Institute.* **2019**, *37*(3), 3135–3142.

[2] M. S. McClain, A. Afriat, J. F. Rhoads, I. E. Gunduz, S. F. Son, Development and Characterization of a Photopolymeric Binder, *Propellants, Explosives, Pyrotechnics.* **2020**, *45*, 853–863.

[3] M. S. Joost van Lingen, C. Van Driel, A. Den Otter, 3D printing of Gun Propellants, *Proceedings of the 43rd International Pyrotechnics Society Seminar*, Fort Collins, CO, USA, July 8–13, **2018**, p. 129–141.

[4] C. Van Driel, M. Straathof, J. Van Lingen, Developments in Additive Manufacturing of Energetic Materials at TNO, *30th International Symposium on Ballistics*, Long Beach, CA, USA, September 11–15, **2017**, p. 862–875.

[5] W. Yang, R. Hu, L. Zheng, G. Yan, W. Yan, Fabrication and investigation of 3D-printed gun propellants, *Materials & Design.* **2020**, *192*, 108761.

[6] R. Hu, W. Yang, Z. Jiang, X. Yu, Q. Wang, 3D Printing Method of Gun Propellants Based on Vat Photopolymerization, *Chinese Journal of Explosives & Propellants.* **2020**, *43(4)*, 368–371.

[7] N. V. Muravyev, K. A. Monogarov, U. Schaller, I. V. Fomenkov, A. N. Pivkina, Progress in additive manufacturing of energetic materials: Creating the reactive microstructures with high potential of applications, *Propellants, Explosives, Pyrotechnics.* **2019**, *44*(8), 941–969.

[8] M. E. Colclough, H. Desai, R. W. Millar, N. C. Paul, M. J. Stewart, P. Golding, Energetic polymers as binders in composite propellants and explosives, *Polymers for Advanced Technologies.* **1994**, *5*(9), 554–560.

[9] D. M. Badgujar, M. B. Talawar, V. E. Zarko, P. P. Mahulikar. New directions in the area of modern energetic polymers: An overview, *Combustion, Explosion, and Shock Waves.* **2017**, *53*(4), 371–387.

[10] A. M. Kawamoto, J. A. S. Holanda, U. Barbieri, G. Polacco, T. Keicher, H. Krause, M. Kaiser, Synthesis and Characterization of Glycidyl Azide-r-(3, 3-bis (azidomethyl) oxetane) Copolymers, *Propellants, Explosives, Pyrotechnics* **2008**, *33*(5), 365–372.

[11] J. K. Nair, R. S. Satpute, B. G. Polke, T. Mukundan, S. N. Asthana, H. Singh, Synthesis and characterisation of bis-azido methyl oxetane and its polymer and copolymer with tetrahydrofuran, *Defence Science Journal* **2002**, *52*(2), 147.

[12] D. M. Badgujar, M. B. Talawar, S. N. Asthana, P. P. Mahulikar, Advances in science and technology of modern energetic materials: an overview, *Journal of Hazardous Materials* **2008**, *151*(2-3), 289–305.

[13] A. Kanti Sikder, S. Reddy, Review on energetic thermoplastic elastomers (ETPEs) for military science, *Propellants, Explosives, Pyrotechnics.* **2013**, *38*(1), 14–28.

[14] Y. L. Sun, Study on Process Adaptability of Energetic Material in Additive Manufacturing by Solvent Method, Nanjing University of Science & Technology, Nanjing, China **2017**.

[15] M. L. Zhou, F. Q. Nan, W. D. He, M. R. Wang, Design and Preparation of Propellant 3D Printer Based on Extrusion Deposition Technology, *Chinese Journal of Energetic Materials.* **2021**, *29*, 530–534.

[16] U. Schaller, D. Mitro, J. Böhnlein-Mauß, T. Keicher, Investigations of ETPE formulations for additive manufacturing, *50th International Annual Conference of ICT*, Karlsruhe, Germany, June 25–28, **2019**, p. 115.

[17] M. H. Straathof, C. A. van Driel, J. N. van Lingen, B. L. Ingenhut, A. T. ten Cate, H. H. Maalderink, Development of Propellant Compositions for Vat Photopolymerization Additive Manufacturing, *Propellants, Explosives, Pyrotechnics.* **2020**, *45*(1): 36–52.

[18] M. H. Straathof, C. A. van Driel, A. T. ten Cate, Energetic materials, International Publication Number WO2017164731 A1. 28 09 **2017**. https://patents.glgoo.top/patent/WO2017164731A1/en.

[19] C. A. Van Driel, D. Ravindre Ramlal, M. Zebregs; M. H. Straathof, Propellant Charge, International Publication Number WO 2017/043975 Al. 16 03 **2017**. https://patents.glgoo.top/patent/WO2017043975A1/en.

[20] M. H. Straathof; C. A. van Driel, Propellant charge or grain, International Publication Number WO2017164732 A1. 28 09 **2017**. https://patents.glgoo.top/patent/WO2017164732A1/en.

[21] S. Sevilia, M. Yong, D. Grinstein, L. Gottlieb, Y. Eichen, Novel, Printable Energetic Polymers, *Macromolecular Materials and Engineering.* **2019**, *304*(6), 1900018.

[22] M. Li, W. Yang, M. Xu, R. Hu, L. Zheng, Study of photocurable energetic resin based propellants fabricated by 3D printing, *Materials & Design.* **2021**, *207*, 109891.

[23] H. E. Kissinger, Reaction kinetics in differential thermal analysis, *Analytical Chemistry*, **1957**, *29*(*11*), 1702–1706.

[24] ASTM E698, American Society for Testing Materials, West Conshohocken, PA, USA.

[25] H. C. Mo, X. X. Gan, Y. Xing, N. Li, Synthesis and properties of energetic binder PNIMMO, *Chinese Journal of Explosives & Propellants.* **2008**;*31*(5), 24–7.

[26] Q. Dong, H. Li, X. Liu, C. Huang, Thermal and rheological properties of PGN, PNIMMO and P(GN/NIMMO) synthesized via mesylate precursors, *Propellants, Explosives, Pyrotechnics.* **2018**, *43*(3), 294–299.

[27] C. Hai, The Investigation of Thermal Decomposition Kinetics for PNIMMO by TG-MS, *Initiators and Pyrotechnics.* **2007**, *2*(4), 32–35.

[28] J. Akhavan, E. Koh, S. Waring, E. Kronfli, Effect of UV and thermal radiation on polyNIMMO, *Polymer* **2001**, *42*(18), 7711–7718.

Manuscript received: August 22, 2021
Revised manuscript received: October 10, 2021
Version of record online: November 8, 2021

